

Clinical Cancer Research



Development of [^{11}C]erlotinib Positron Emission Tomography for *In Vivo* Evaluation of EGF Receptor Mutational Status

Idris Bahce, Egbert F. Smit, Mark Lubberink, et al.

Clin Cancer Res 2013;19:183-193. Published OnlineFirst November 7, 2012.

Updated Version

Access the most recent version of this article at:
doi:[10.1158/1078-0432.CCR-12-0289](https://doi.org/10.1158/1078-0432.CCR-12-0289)

Supplementary Material

Access the most recent supplemental material at:
<http://clincancerres.aacrjournals.org/content/suppl/2012/11/06/1078-0432.CCR-12-0289.DC1.html>

Cited Articles

This article cites 22 articles, 6 of which you can access for free at:
<http://clincancerres.aacrjournals.org/content/19/1/183.full.html#ref-list-1>

E-mail alerts

[Sign up to receive free email-alerts](#) related to this article or journal.

Reprints and Subscriptions

To order reprints of this article or to subscribe to the journal, contact the AACR Publications Department at pubs@aacr.org.

Permissions

To request permission to re-use all or part of this article, contact the AACR Publications Department at permissions@aacr.org.

Development of [^{11}C]erlotinib Positron Emission Tomography for *In Vivo* Evaluation of EGF Receptor Mutational Status

Idris Bahce¹, Egbert F. Smit¹, Mark Lubberink², Astrid A. M. van der Veldt², Maqsood Yaqub², Albert D. Windhorst², Robert C. Schuit², Erik Thunnissen³, Daniëlle A. M. Heideman³, Pieter E. Postmus¹, Adriaan A. Lammertsma², and N. Harry Hendrikse^{2,4}

Abstract

Purpose: To evaluate whether, in patients with non-small cell lung carcinoma (NSCLC), tumor uptake of [^{11}C]erlotinib can be quantified and imaged using positron emission tomography and to assess whether the level of tracer uptake corresponds with the presence of activating tumor EGF receptor (EGFR) mutations.

Experimental Design: Ten patients with NSCLCs, five with an EGFR exon 19 deletion, and five without were scanned twice (test retest) on the same day with an interval of at least 4 hours. Each scanning procedure included a low-dose computed tomographic scan, a 10-minute dynamic [^{15}O]H₂O scan, and a 1-hour dynamic [^{11}C]erlotinib scan. Data were analyzed using full tracer kinetic modeling. EGFR expression was evaluated using immunohistochemistry.

Results: The quantitative measure of [^{11}C]erlotinib uptake, that is, volume of distribution (V_T), was significantly higher in tumors with activating mutations, that is, all with exon 19 deletions (median V_T , 1.76; range, 1.25–2.93), than in those without activating mutations (median V_T , 1.06; range, 0.67–1.22) for both test and retest data ($P = 0.014$ and $P = 0.009$, respectively). Good reproducibility of [^{11}C]erlotinib V_T was seen (intraclass correlation coefficient = 0.88). Intergroup differences in [^{11}C]erlotinib uptake were not correlated with EGFR expression levels, nor tumor blood flow.

Conclusion: [^{11}C]erlotinib V_T was significantly higher in NSCLCs tumors with EGFR exon 19 deletions. *Clin Cancer Res*; 19(1); 183–93. ©2012 AACR.

Introduction

In the Western population, approximately 10% of patients with non-small cell lung carcinoma (NSCLC) harbor an activating mutation in their tumor EGF receptor (EGFR) genes. The most common activating EGFR mutations are exon 19 deletions (particularly delE746–A750) and exon 21 point mutations (particularly L858R; refs. 1, 2). Proper identification of these patients, usually presenting with advanced stage disease, is of clinical importance, as recent trials have shown that treatment with EGFR tyrosine

kinase inhibitors (TKI), such as erlotinib or gefitinib, results in a high response rate and significantly longer progression-free survival (PFS) than treatment with classical cytotoxic chemotherapy (3–5).

Identifying patients with activating mutations, however, remains a major clinical challenge. Obtaining representative tumor tissue samples for mutation analysis is often limited by practical issues, such as inability to reach the tumor site, low yields of malignant cells, or tumor heterogeneity. Indeed, results of recent clinical trials have shown that tissue procurement may not be possible in more than one fifth of patients (6). A noninvasive technique may overcome the obstacles associated with tumor tissue sampling. For this, positron emission tomography (PET), which allows for *in vivo* imaging of physiologic processes, seems to be best suited.

Compared with NSCLC tumors with wild-type EGFR, those with activating EGFR mutations have higher TKI binding affinity (7). Therefore, uptake of radiolabeled TKI may be higher in tumors with activating EGFR mutations. In the present study, [^{11}C]erlotinib, chemically identical to erlotinib itself, was used. Imaging of TKI-sensitive tumor xenografts has already been shown in an *in vivo* model using this tracer (8).

Authors' Affiliations: Departments of ¹Pulmonary Diseases, ²Nuclear Medicine & PET Research, ³Pathology, and ⁴Clinical Pharmacology & Pharmacy, VU University Medical Center, Amsterdam, Netherlands

Note: Supplementary data for this article are available at Clinical Cancer Research Online (<http://clincancerres.aacrjournals.org/>).

Current address for M. Lubberink: PET Centre, Uppsala University Hospital, Uppsala, Sweden.

Corresponding Author: Idris Bahce, Department of Pulmonary Diseases 4A48, VU University Medical Center, PO Box 7057, Amsterdam 1007 MB, Netherlands. Phone: 31-20-4444782; Fax: 31-20-4444328; E-mail: i.bahce@vumc.nl

doi: 10.1158/1078-0432.CCR-12-0289

©2012 American Association for Cancer Research.

Translational Relevance

In the present study, uptake and tumor kinetics of [^{11}C]erlotinib in patients with non-small cell lung carcinoma (NSCLC) with and without EGFR receptor (EGFR) exon 19 deletions were quantified using a newly developed tracer kinetic model. Patients harboring EGFR exon 19 deletions showed higher tumor uptake of [^{11}C]erlotinib than in patients without activating EGFR mutations. This is of potential clinical importance, as it provides evidence that tyrosine kinase inhibitor (TKI)-sensitive tumors, harboring EGFR exon 19 deletions, may be identified by [^{11}C]erlotinib positron emission tomography (PET). Patients with activating EGFR mutations need to be treated with TKI in a first-line setting, contrary to patients without EGFR mutations who are best treated with cytotoxic chemotherapy. [^{11}C]erlotinib and PET may potentially be a noninvasive means for identifying patients with NSCLCs who may benefit from TKI therapy.

Although [^{11}C]erlotinib has been used to image NSCLC tumors in a limited number of patients, no quantitative analysis has been described (9, 10). Quantification, however, is essential for an objective comparison of uptake in different tumors. Therefore the aims of the present study were to develop the optimal tracer kinetic model and its corresponding measure for quantification of [^{11}C]erlotinib uptake in NSCLCs, to determine its reproducibility, and to assess whether tumor uptake of [^{11}C]erlotinib correlates with EGFR mutational status.

Materials and Methods

Study design

This study consisted of a number of distinct steps. Patients with and without an activating EGFR mutation underwent 2 dynamic [^{11}C]erlotinib PET scans with continuous arterial blood sampling on the same day. Each [^{11}C]erlotinib scan was preceded by a [^{15}O]H₂O scan to assess tumor blood perfusion. First, [^{11}C]erlotinib data from all patients, including test-retest information, were used to determine the optimal model for describing erlotinib kinetics. This model was used to assess whether there were differences between tumors with and without activating EGFR mutations. Finally, validity of a noninvasive image derived input function was evaluated in an attempt to simplify the protocol for routine clinical applications.

Patients

Ten patients with NSCLCs were included, 5 with and 5 without an activating mutation. Inclusion criteria were histologic diagnosis of NSCLCs, EGFR mutational status as assessed by high resolution melting (HRM), and sequencing of tumor biopsies (11, 12), EGFR expression as determined by immunohistochemistry (IHC), an age of 18 years or older, a life expectancy of at least 12 weeks, presence of a

malignant lesion within the chest of at least 1.5 cm diameter as measured by computed tomography (CT), and written informed consent. Exclusion criteria were claustrophobia, pregnancy, lactation, metal implants in the thorax, and use of concurrent or previous treatment with experimental drugs within 30 days before scanning. The study was approved by the Medical Ethics Review Committee of the VU University Medical Center.

Synthesis of [^{11}C]erlotinib

[^{11}C]erlotinib was synthesized under GMP conditions according to the EU directive on radiopharmaceuticals, EudraLex - Volume 4. The precursor was custom synthesized at Syncom. The carbon-11 label was introduced at the 7-methoxyethoxy position of the precursor, 6-*O*-desmethyl-erlotinib (OSI 420), using [^{11}C]methyl iodide (Supplementary Fig. S1). [^{11}C]methyl iodide was synthesized from [^{11}C]CO₂ according to standard procedures and subsequently distilled in a solution of the precursor in acetonitrile and tetra-*n*-butylammonium hydroxide. The maximum yield was obtained after 5 minutes at 80°C. After cooling down and dilution with 0.75 mL of water, the mixture was injected onto a Waters SymmetryPrep C18 7 μm 300 \times 7.8 mm HPLC column, which was eluted with 70/30 25 mmol/L phosphate buffer (pH 3.5)/acetonitrile mixture. The product, [^{11}C]erlotinib, eluted at 9.5 minutes. This fraction was collected in 20 mL of water for injection. The total solution was passed over a preconditioned (10 mL of sterile ethanol 96% and subsequently 10 mL of water for injection) Waters Sep-Pak tC18 cartridge. This cartridge was washed with 20 mL of water for injection and subsequently the product was eluted from the cartridge with 1.0 mL of sterile ethanol (96%) and 14 mL of a sterile and pyrogen-free solution of 7.1 mmol/L NaH₂PO₄ saline. The final mixture was passed over a Millex GV 0.22 μm filter, yielding a sterile, isotonic and pyrogen-free solution of 2183-3476 MBq of [^{11}C]erlotinib with a (radio)chemical purity more than 98% and a specific activity of 184-587 GB/ μmol at end of synthesis ($n = 20$). The product was analyzed using HPLC with a Phenomenex LUNA C18 5 μm 250 \times 4.6 mm column, which was eluted with 55/45 acetonitrile/saline.

PET-CT scanning

All patients underwent 2 scanning sessions on the same day, with an interval of at least 4 hours to allow for radioactive decay of carbon-11. Scans were conducted on a Gemini TF-64 PET/CT scanner (Philips Medical Systems). PET data were normalized and all appropriate corrections were applied for dead time, decay, randoms, scatter, and attenuation. Reconstruction of PET data was conducted using the 3-dimension (3D) RAMLA algorithm with CT-based attenuation correction, resulting in a final voxel size of 4 \times 4 \times 4 mm³ and a spatial resolution of 5 to 7 mm full width at half maximum. Before scanning, all patients were asked to fast from midnight, but a light breakfast before 8:00 am was allowed. First, a low-dose CT scan (50 mAs, without i.v. or oral contrast) was conducted. To assess tumor

perfusion, 370 ± 37 MBq (mean \pm SD) [¹⁵O]H₂O was injected intravenously, simultaneously starting a 10-minute emission scan in 3D acquisition mode. Subsequently 256 ± 53 MBq (mean \pm SD) [¹¹C]erlotinib (corresponding to a nonpharmacologic dose of 2.2 ± 0.46 μ g erlotinib) was injected intravenously, simultaneously starting a 60-minute emission scan in 3D acquisition mode. [¹⁵O]H₂O and [¹¹C]erlotinib emission scans were acquired in list mode and, before reconstruction, sorted into 26 (1×10 , 8×5 , 4×10 , 2×15 , 3×20 , 2×30 , and 6×60 seconds) and 36 (1×10 , 8×5 , 4×10 , 2×15 , 3×20 , 2×30 , 6×60 , 4×150 , 4×300 , and 2×600 seconds) frames with increasing frame duration, respectively. No corrections for patient motion and/or respiratory motion were applied.

Arterial blood sampling

An indwelling cannula was inserted in the radial artery for arterial blood sampling. No blood was withdrawn during [¹⁵O]H₂O PET scans, as it has previously been shown that these scans can be quantified using an image-derived input function (13). During the [¹¹C]erlotinib PET scans, arterial blood was withdrawn continuously at a rate of 5 mL/min for the first 5 minutes followed by 1 mL/min for an additional 35 minutes. This was monitored using an online detection system (Veenstra Instruments), cross-calibrated against the PET scanner (14). In addition, manual arterial samples (7 mL) were taken at 2.5, 5, 10, 15, 20, 30, 40, and 60 minutes after injection of [¹¹C]erlotinib. These discrete samples were used for calibration of the online arterial curve and for measuring plasma-to-whole blood ratios and radiolabeled plasma parent and metabolite fractions as function of time.

Metabolite analysis

Manual blood samples were analyzed for blood and plasma radioactivity concentrations and for radiolabeled fractions (i.e., parent and both polar and nonpolar metabolites) of [¹¹C]erlotinib. Whole blood (0.5 mL) was weighted in duplicate and after centrifuging (5 minutes; 7°C; 4,000 rpm.), plasma was harvested and 0.5 mL plasma was weighted in duplicate. A well-counter, cross-calibrated against the PET scanner was used to determine activity concentrations in whole blood and plasma.

To determine the fractions of [¹¹C]erlotinib and its labeled metabolites in each sample, solid-phase extraction (SPE) and high-performance liquid chromatography (HPLC) were used. About 1 mL of plasma was diluted with 2 mL of water and loaded onto an activated Waters Sep-Pak tC2 SPE column. To separate the parent compound from its metabolites, an HPLC system was used. The eluate was injected onto a Phenomenex Gemini 5 μ m 250 \times 10 mm with a flow of 3 mL/min. The gradient system was a mixture of acetonitrile (A) and 10 mmol/L ammonium acetate (B) and was programmed as following: $t = 0$ minute 90% B, $t = 15$ minutes 30% B, $t = 20$ minutes 30% B, $t = 21$ minutes 90% B, $t = 25$ minutes 90% B. Fractions were collected and measured for radioactivity with a gamma-counter to generate an HPLC profile.

Region of interest definition

First, images were converted to ECAT7 format. Regions of interest (ROI) were drawn manually within (i.e., smaller than) tumor contours on the CT images, avoiding blood vessels and necrosis as much as possible, using CAPP software (CTI/Siemens), and subsequently projected onto the corresponding PET images. CAPP software was also used to generate tumor time-activity curves (TAC) for all tumor ROI of both [¹⁵O]H₂O and [¹¹C]erlotinib scans.

Pharmacokinetic analysis of [¹¹C]erlotinib data

Pharmacokinetic modeling was performed using in-house software, developed within the Matlab (The MathWorks Inc.) environment. First, using standard nonlinear regression techniques, tumor [¹¹C]erlotinib TAC were fitted to different (i.e., 1-tissue, irreversible 2-tissue, and reversible 2-tissue) compartment models (15) using the measured metabolite corrected plasma time-activity curve as input function. The optimal model was selected on the basis of both Akaike Information and Schwarz Criteria (16, 17). For the 1-tissue compartment model, the outcome measure of tracer uptake is the volume of distribution V_T , and for the irreversible 2-tissue compartment model, it is the influx rate constant K_i . In case of the reversible 2-tissue compartment model, both V_T and the nondisplaceable binding potential (BP_{ND}) can be used as outcome parameters. The most appropriate parameter was chosen depending on test-retest variability. When fitting to the different compartment models, a blood volume parameter was included to correct for the intravascular contribution to the signal.

Image-derived input function

A less invasive alternative to using continuous arterial blood sampling in [¹¹C]erlotinib kinetic analyses is the use of an image-derived input function (IDIF), however, results obtained with IDIF need to be validated against full arterial sampling. IDIF reflects the activity concentration in plasma over time and is derived from dynamic PET data of the arterial blood pool. To generate IDIF, ROIs were drawn within the ascending aorta of early [¹¹C]erlotinib frames (typically 30 to 35 seconds after injection) in 10 successive slices, resulting in an approximate volume of 6.3 mm³. By multiplying the arterial whole blood TAC derived from the aorta ROI with a multiexponential function, derived from the best fit to the plasma-to-whole blood radioactivity ratios of the discrete arterial samples, a plasma TAC was obtained. Then, the plasma TAC was corrected for metabolites using a sigmoid function derived from the best fit to the measured parent fractions of the arterial samples. Finally, this metabolite corrected plasma TAC was used as IDIF (18).

Analysis of tumor perfusion

Using nonlinear regression, tumor [¹⁵O]H₂O TACs were processed according to the standard single tissue compartment model with IDIF as input function, as described previously (13). This analysis generated blood flow (F) values, reflecting tumor perfusion (mL/cm³/min).

Mutation analysis

Mutation analysis of EGFR was conducted using HRM and sequencing, as described previously (11, 12).

Immunohistochemistry

EGFR protein expression intensity was determined using IHC and scored visually, that is, semiquantitatively, as described previously (19).

Tumor response evaluation

Response during erlotinib treatment was measured using Response Evaluation Criteria in Solid Tumors (RECIST; ref. 20).

Statistical analysis

Statistical analysis was conducted using SPSS software (SPSS for Windows 15.0, SPSS, Inc.). Level of agreement between test and retest scans was determined using the intraclass correlation coefficient (ICC) with a 2-way random-effects model. Values for the ICC range from 0 to 1. Values close to 0 indicate poor agreement between test and retest scans, whereas values close to 1 indicate high agreement. ICC values above 0.70 are considered to have good reproducibility. In addition, the Mann-Whitney test was used to compare V_T and tumor perfusion (F) values between patient groups with and without activating EGFR mutations. Correlations were explored using the Spearman correlation coefficient (r_s). A 2-tailed probability value of $P < 0.05$ was considered significant. EGFR mutational status was known for all patients before kinetic analysis.

Results

Patients' characteristics

Baseline characteristics of all patients are shown in Table 1. Patients were divided into 2 groups. Group 1 consisted of patients with NSCLCs without activating EGFR mutations. Patient 5 in this group was diagnosed with an adenocarcinoma, harboring only an exon 20 insertion [D770-N771 (ins GG) + N771T]. This is a rare primary oncogenic mutation, insensitive to erlotinib, not considered to be an activating EGFR mutation, and thus classified in group 1 (21). All other patients in this group had a wild-type tumor EGFR. All patients in group 2 had an exon 19 deletion. High EGFR expression in all tumor cells, as assessed by IHC, was reported for 4 out of 5 tumors in group 1 and for all tumors in group 2. Examples are shown in Fig. 1.

Except for one, all patients underwent 2 scan sessions for a total of 19 [^{11}C]erlotinib scans. Patient 9 in group 2 missed the first [^{11}C]erlotinib scan due to technical problems with the arterial cannula.

Treatment characteristics

Before this study, 5 patients had been treated with TKI. In group 1, patients 3 and 4 had received TKI as second-line therapy without experiencing any tumor response. In group 2, patients 7 and 10 initially had achieved a partial response on TKI, but treatment was discontinued because of drug

toxicity and disease progression, respectively. Patient 8 achieved an initial partial response on TKI for almost a year. Upon first disease progression, she was treated with cytotoxic chemotherapy showing a partial response. After a second progression, she restarted TKI therapy, this time without tumor response (see Table 1).

After the [^{11}C]erlotinib study, none of the patients in group 1 and 3 patients in group 2 started treatment with TKIs. Patient 6 was treated with TKI for the first time, whereas patients 7 and 10 were treated again. All achieved a partial response. Patients 6 and 10 maintained this partial response for 18 and 4 months, respectively. To date, 20 months after start of treatment, patient 7 still has a partial response (see Table 1).

Pharmacokinetic analysis of [^{11}C]erlotinib data

Tumor sizes ranged from approximately 5 to 100 mm³, with tumor ROI, drawn inside the tumor contours, varying between 2.4 to 91.4 mm³. Analysis of tumor TAC, using both Akaike and Schwarz criteria, showed that the reversible 2-tissue model provided the best fits in 15 of 19 scans. Therefore, further analyses were conducted using this model only. Figure 2 shows fits to a typical tumor TAC using the 3 plasma input models investigated. Fits for all different compartment models were corrected for intravascular activity by including a blood volume parameter. These blood volume fractions were non-zero in most patients (median 0.06; range, 0–0.40) for the defined ROI.

This model provides 2 potential parameters of interest, V_T and BP_{ND} . V_T was selected as outcome measure because of its superior test–retest variability (ICC for V_T and BP_{ND} were 0.88 (95% confidence interval, CI, 0.55–0.97) and –0.02 (95% CI, –0.64 to 0.62), respectively]. V_T results are shown in Table 2.

V_T of [^{11}C]erlotinib was higher in tumors with EGFR exon 19 deletions than in tumors without activating EGFR mutations. This result was found both for test and retest scans ($P = 0.014$ and $P = 0.009$, respectively; Table 2). Patient 9 in group 2 had a higher fitting error, which was probably due to the presence of lymphoid tissue in the tumor ROI. Representative parametric [^{11}C]erlotinib images, using Logan analysis over the interval 20 to 60 minutes (22), of patients with NSCLCs with wild-type and mutated EGFR are shown in Fig. 3.

V_T values obtained with metabolite-corrected IDIF (Table 2) correlated well with those obtained with full arterial sampling ($r_s = 0.96$, $P < 0.001$), considered to be gold standard, as indicated in Fig. 4. Using IDIF data, tumors with EGFR exon 19 deletions also had significantly higher V_T values than those without for both test and retest scans ($P = 0.014$ and $P = 0.009$, respectively). The test–retest variability (ICC = 0.85; 95% CI, 0.46–0.96) was similar as obtained with full arterial sampling.

Plasma analysis

The parent fraction in groups 1 and 2, indicating unchanged [^{11}C]erlotinib in plasma, steadily decreased to $54\% \pm 2\%$ and $43\% \pm 7\%$ (mean \pm SD) at 60 minutes after

Table 1. Patient and treatment characteristics

Group	Patient number	Patient characteristics	Stage (TNM)	Biopsy	Erlotinib therapy
		• Age • Sex • Smoking status • Ethnicity		• Time until PET scan • Histology • IHC • EGFR DNA sequencing	• TKI before PET scan ^a • TKI after PET scan ^b
1	1	• 61 • Male • Former smoker • Caucasian	IIIb (cT4Nx-2M0)	• 20 d • ASC • +++ • Wild-type	• NA • NA
1	2	• 57 • Male • Former smoker • Caucasian	IIIb (cT4Nx-2M0)	• 4 mo after PET scan • SCC • +++ • Wild-type	• NA • NA
1	3	• 59 • Female • Former smoker • Caucasian	IV (cT4N2M1a)	• 20 mo • AC • +++ • Wild-type	• 2 mo/PD/3 mo • NA
1	4	• 46 • Female • Never smoker • African	IV (cT4N2M1a)	• 16 mo • AC • ++ • Wild-type	• 4 mo/PD/41 mo • NA
1	5	• 65 • Male • Former smoker • Caucasian	IV (rT2aN1M1a)	• 28 mo • AC • +++ • Exon 19 wild-type; exon 20 insertion (D770–N771 (ins GG) + N771T)	• NA • NA
2	6	• 46 • Female • Never smoker • Asian	IIIb (cT4N3M0)	• 13 d • AC • +++ • Exon 19 deletion (del E746–A750)	• NA • 18 mo/PR/1 d
2	7	• 47 • Male • Never smoker • Asian	IV (cT3N0M1a)	• 1 mo • AC • +++ • Exon 19 deletion (del L747–T751)	• 19 mo/PR/4 mo • 20 mo ^c /PR/3 wk
2	8	• 51 • Female • Never smoker • Caucasian	IV (T2aN3M1b)	• 6 d • ASC • +++ • Exon 19 deletion (del E746–A750)	• First episode ^d : 11 mo/PR • Second episode: 3 mo/PD/3 wk • NA
2	9	• 37 • Female • Never smoker • Caucasian	IIa (rT1N1M0)	• 10 mo • AC • +++ • Exon 19 deletion (del E746–A750)	• NA • NA ^e
2	10	• 54 • Female • Never smoker • Caucasian	IV (T4N0M1a)	• 12 mo • AC • +++ • Exon 19 deletion (del E746–A750)	• 18 mo/PR/11 mo • 4 mo/PR/1 d

NOTE: Patients were categorized into 2 groups, according to the presence of activating mutations. Disease stage is indicated using the IASLC classification, 7th edition (25). Using IHC, EGFR protein expression was visually scored as high (+++), moderate (++), or low (+; ref. 19). EGFR mutational status was assessed by DNA sequencing on tumor biopsies (11, 12).

Abbreviations: AC, adenocarcinoma; ASC, adenosquamous carcinoma; NA, not applicable; PD, progressive disease; PR, partial response; SCC, squamous cell carcinoma.

^aErlotinib therapy duration, best response, and TKI-free period for patients treated before scanning are shown.

^bTreatment duration, best response, and start date of erlotinib for patients treated after scanning are shown. Best response to TKI therapy prior and after scanning was scored according to RECIST (20).

^cPatient 7 is progression free to date, that is, 22 months and ongoing.

^dPatient 8 was treated twice with erlotinib: in a first episode, she achieved partial response, but treatment was discontinued after 11 months due to disease progression. Six months after discontinuation she was retreated with erlotinib, this time she did not achieve tumor response.

^ePatient 9 was treated with chemoradiation, not with TKI, as this patient had only local disease.

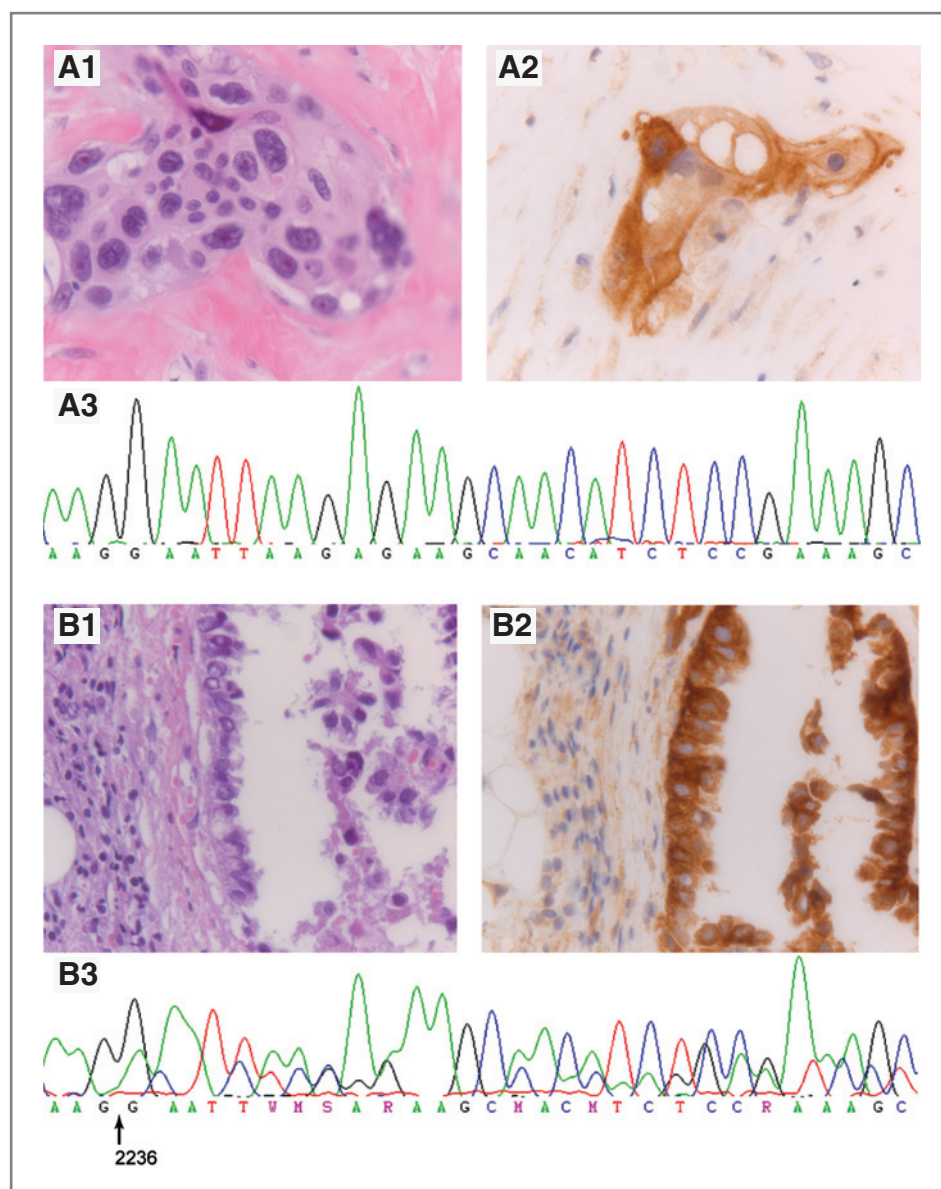


Figure 1. Images obtained from tumor biopsy (at $\times 40$ objective) of patient 2, stained with (A1) hematoxylin and eosin (H&E) and (A2) EGFR IHC (19) and of patient 6, stained with (B1) H&E and (B2) EGFR IHC. EGFR DNA sequences c.2233 through c.2264 are shown from the above mentioned patients with respectively (A3) wild-type EGFR and (B3) an exon 19 deletion (c.2236_2250del15; p.del E746-A750; start of the deletion is indicated by \uparrow). The nucleic acid coordinates used to name the EGFR mutations are based on RefSeq sequence NM_005228.3.

injection, whereas polar radiolabeled metabolites steadily increased over 60 minutes to $31\% \pm 21\%$ and $33\% \pm 17\%$, respectively. The fraction of nonpolar metabolites, as assessed by HPLC, was too small to be quantified reliably. Therefore, use of SPE only (i.e., measuring polar metabolites) was sufficient. Results for wild-type and mutated EGFR patients are shown in Supplementary Fig. S2. The fractions do not add up to 100%, because not all blood samples could be measured in all subjects.

Perfusion

Because of technical problems, only one $[^{15}\text{O}]\text{H}_2\text{O}$ scan was conducted in patients 2 and 9. There was no difference in tumor blood flow between both groups, with P values of 0.111 and 0.413 for test ($n = 9$) and retest ($n = 9$) scans, respectively. There was good test-retest consistency (ICC =

0.81, Table 2). Average $[^{11}\text{C}]\text{erlotinib } K_1$ values for wild-type and mutated EGFR were not significantly different ($P = 0.372$) with 0.30 (SD = 0.29) and 0.44 (SD = 0.13), respectively. Correlation between K_1 and flow was good ($r_s = 0.70$, $P = 0.031$).

Discussion

Pharmacokinetic modeling using arterial sampling

The aim of this study was to develop a method to quantify $[^{11}\text{C}]\text{erlotinib}$ uptake in NSCLC tumors, which could be used as an *in vivo* tool for detecting activating EGFR mutations. For quantification of PET tracer studies, the gold standard is kinetic modeling using a measured metabolite-corrected arterial plasma curve as input function. Using this approach, best fits were obtained with the reversible 2-tissue compartment model, providing volume of distribution (V_T)

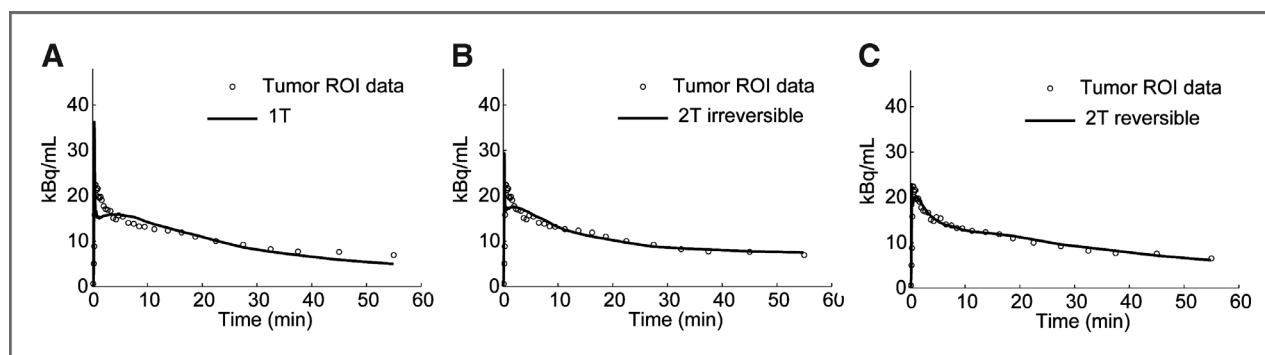


Figure 2. Tumor [¹¹C]erlotinib TAC (open circles) with best fits according to (A) 1-tissue, (B) irreversible 2-tissue, and (C) reversible 2-tissue compartment models. The latter fit describes the measured PET data best.

as a measure of [¹¹C]erlotinib uptake. The test–retest design of the present study showed that [¹¹C]erlotinib V_T values were reproducible (Table 2). This model was used in all further analyses.

Pharmacokinetic modeling using IDIF

[¹¹C]erlotinib V_T values obtained using IDIF correlated well with V_T obtained using arterial sampling (Fig. 4). Reproducibility of IDIF based [¹¹C]erlotinib V_T values was also good for all patients (Table 2). These findings validate the use of IDIF in future studies, making this technique better suitable for routine clinical use. Although continuous

arterial sampling can now be omitted, image derived whole blood curves still need to be corrected for both plasma-to-whole blood radioactivity ratios and the fraction of radiolabeled metabolites. Even though this needs to be confirmed for [¹¹C]erlotinib, these measurements may be obtained from a number of discrete venous rather than arterial samples, as shown in studies using other tracers (23).

EGFR mutational status

Unintentionally only patients with exon 19 deletions, and no patients with other activating mutations, such as

Table 2. Fitted V_T of [¹¹C]erlotinib and perfusion values with associated SEs (of the fit)

N	EGFR	V_T of [¹¹ C]erlotinib \pm SE (unitless)				Perfusion \pm SE (mL/cm ³ /min ¹)	
		Sampler ^a		IDIF ^b		Scan 1	Scan 2
		Scan 1	Scan 2	Scan 1	Scan 2		
1	WT	1.12 \pm 0.20	0.90 \pm 0.01	0.99 \pm 0.11	0.90 \pm 0.04	0.36 \pm 0.02	0.30 \pm 0.04
2	WT	0.67 \pm 0.01	0.67 \pm 0.04	0.69 \pm 0.01	0.69 \pm 0.02	0.34 \pm 0.02	NA
3	WT	1.22 \pm 0.37	1.17 \pm 0.12	1.31 \pm 0.36	1.27 \pm 0.14	0.33 \pm 0.02	0.33 \pm 0.02
4	WT	1.09 \pm 0.02	1.18 \pm 0.02	1.11 \pm 0.02	1.17 \pm 0.02	0.65 \pm 0.03	0.67 \pm 0.03
5	Ins Ex20	0.90 \pm 0.04	1.03 \pm 0.04	0.89 \pm 0.04	1.20 \pm 0.26	0.43 \pm 0.04	0.42 \pm 0.03
6	Ex19del	1.30 \pm 0.02	1.76 \pm 0.02	1.33 \pm 0.03	1.90 \pm 0.04	0.48 \pm 0.01	0.57 \pm 0.02
7	Ex19del	1.84 \pm 0.07	2.16 \pm 0.10	1.90 \pm 0.10	2.20 \pm 0.12	0.56 \pm 0.02	0.46 \pm 0.01
8	Ex19del	1.27 \pm 0.07	1.25 \pm 0.05	1.33 \pm 0.07	1.42 \pm 0.07	0.57 \pm 0.05	0.65 \pm 0.04
9	Ex19del	NA	2.93 \pm 0.94	NA	2.35 \pm 0.50	NA	0.31 \pm 0.04
10	Ex19del	1.57 \pm 0.06	1.77 \pm 0.06	2.22 \pm 1.50	1.85 \pm 0.07	1.29 \pm 0.09	2.07 \pm 0.17
Test vs. retest		ICC = 0.88 (95% CI, 0.55–0.97), $P < 0.001$		ICC = 0.85 (95% CI, 0.46–0.96), $P = 0.001$		ICC = 0.81 (95% CI, 0.32–0.96), $P = 0.004$	
Mutated vs. nonmutated		Mann–Whitney, 2-tailed		Mann–Whitney, 2-tailed		Mann–Whitney, 2-tailed	
		Scan 1 $P = 0.014$ Scan 2 $P = 0.009$		Scan 1 $P = 0.014$ Scan 2 $P = 0.009$		Scan 1 $P = 0.111$ Scan 2 $P = 0.413$	

NOTE: Scans 1 and 2 refer to test and retest scans.

Abbreviations: NA, not applicable; WT, wild-type.

^aPlasma input based on continuous arterial blood sampling (standard method).

^bIDIF input based on limited blood sampling (less invasive method).

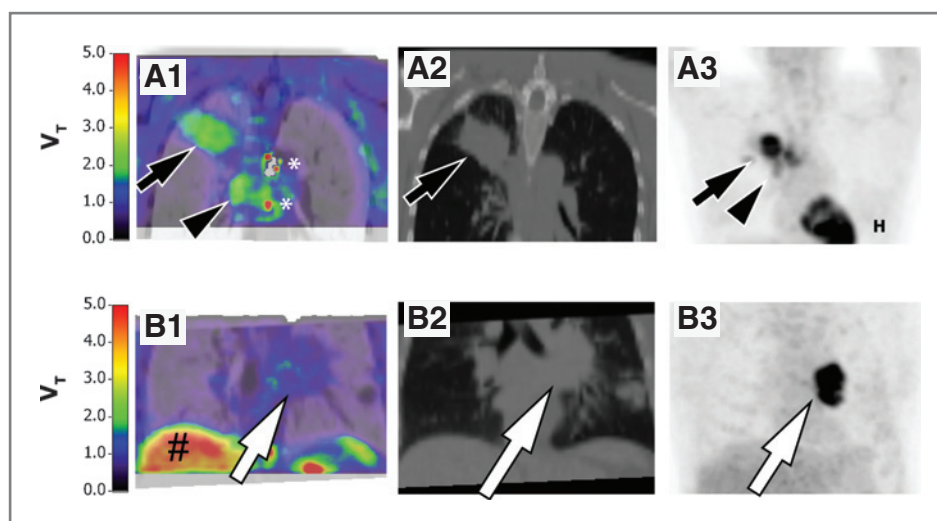


Figure 3. Representative images of 2 different patients with NSCLCs. A, patient 2 with wild-type EGFR, tumor located at the left hilum (white arrow). B, patient 6 with an EGFR exon 19 deletion, tumor in the right upper lobe (black arrow) and mediastinal lymph nodes (black arrowhead). Patient 6 (with mean tumor V_T of 1.30) shows higher tumor uptake than patient 2 (with mean tumor V_T of 0.67) as indicated by the color code. The liver (#) shows physiologic uptake of metabolized and nonmetabolized [^{11}C]erlotinib. *, notice high V_T artifacts caused by mediastinal blood vessels. Coronal images are shown of (A1 and B1) CT-fused parametric [^{11}C]erlotinib V_T , (A2, B2) CT, and (A3, B3) [^{18}F]FDG uptake. H, high FDG uptake is seen in the heart.

L858R, were included in group 2. V_T of [^{11}C]erlotinib, as determined using both arterial sampling and IDIF, was significantly higher in group 2 than in group 1, for both test and retest scans. Although many factors contribute to tumor [^{11}C]erlotinib accumulation in PET, the differences in V_T may be caused by differences in affinity to erlotinib. Erlotinib competes with ATP to bind at the ATP-binding site of the EGFR kinase domain. Kinase assay studies have found values for the erlotinib dissociation constant (K_i) of 3.3, 6.3, and 17.5 nmol/L, and Michaelis-Menten constant (K_M) values for ATP of 129.0, 10.9, and 5.0 $\mu\text{mol/L}$ for exon 19 deletions, exon 21 point mutations and wild-type EGFR, respectively (7). This means that erlotinib affinity is higher

for EGFR with activating mutations than for wild-type EGFR, whereas ATP affinity is lower. Compared with wild-type EGFR, exon 19 deletions and exon 21 mutations exhibit 137-fold and 6-fold higher binding to erlotinib relative to ATP (i.e., K_i/K_M ratios), respectively (7).

Contributing factors

Although high affinity of erlotinib for EGFR represents a favorable parameter for [^{11}C]erlotinib as a PET tracer, differences in K_i/K_M ratios between wild-type and mutated EGFR (i.e., >100-fold for exon 19 deletions) are not reflected in the same magnitude in V_T values (i.e., ~2-fold). Clearly, *in vitro* studies occur in more simplified circumstances than *in vivo* studies, lacking complex interactions, such as nonspecific binding and the presence of radiolabeled metabolites that cause underestimation of V_T differences. In addition, *in vitro* conditions may deviate from normal physiologic conditions. For example, differences in ATP affinity between wild-type EGFR and mutated EGFR are seen at low ATP concentrations, but at higher, near physiologic ATP concentrations, these differences become less significant (7, 24). Other *in vivo* factors may also contribute to the observed differences in tumor [^{11}C]erlotinib uptake, such as EGFR protein expression and blood flow. However, both tumor EGFR protein expression and tumor blood flow were comparable between tumors with and without an EGFR exon 19 deletion.

Erlotinib therapy

In this study, 6 of 10 patients received erlotinib therapy, either before or after scanning. In group 1, only 2 patients were treated with erlotinib. This was before scanning, and none of the 2 low V_T patients achieved tumor response. Three patients in group 2 were treated with erlotinib after

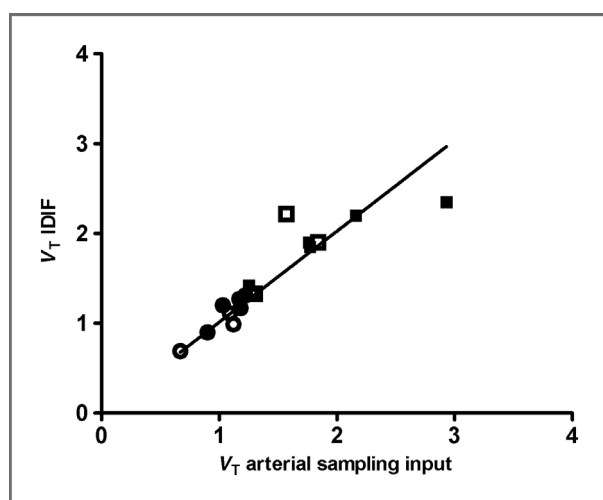


Figure 4. Correlation between V_T values derived from IDIF and those obtained using full arterial sampling. Test ($n = 9$) and retest ($n = 10$) data were pooled. Spearman correlation coefficient = 0.92, $P < 0.01$ (Table 2).

scanning. These 3 high V_T patients achieved a partial response. The remaining patient in group 2 (patient 8) developed resistance to erlotinib, which was diagnosed 3 weeks before her ¹¹C]erlotinib PET. Interestingly, her V_T was higher than in the nonmutated group, but the lowest observed in the mutated group, which could be in accordance with her clinically diminished TKI sensitivity. Although the sample size in this study is too small to draw any definite conclusions, these findings support the hypothesis that increased ¹¹C]erlotinib V_T correlates with tumor response to erlotinib. Clearly, these findings need to be confirmed in larger trials.

Recently, results of a qualitative study on 13 patients undergoing ¹¹C]erlotinib scanning were reported (9). Four patients died before response evaluation. Of the 9 patients who were evaluable for tumor response to erlotinib therapy, all 3 patients with high ¹¹C]erlotinib accumulation showed stable disease, whereas 4 of 6 patients with lower accumulation had progressive disease and the remaining 2 had stable disease. Unfortunately, EGFR mutational status was not measured in this study. Nevertheless, these results also indicate that ¹¹C]erlotinib uptake may predict tumor sensitivity to erlotinib therapy.

Clinical response to TKI depends on EGFR affinity to TKI and ATP but also on oncogene addiction of tumor cells. As, in clinical practice, up to 80% of patients harboring activating EGFR mutations respond to TKI, it could be hypothesized that responders have EGFR-driven growth and nonresponders may have other mechanisms that activate proliferation. Whether tumor growth in a patient is fully driven by the EGFR pathway cannot be measured using ¹¹C]erlotinib PET.

Study limitations

This study has a number of limitations. First, being a proof-of-concept study, only a limited number of patients were included. According to the inclusion criteria, all activating EGFR mutations, including exon 19 deletions and exon 21 point mutations, were allowed to enter group 2. Unintentionally, only patients with exon 19 deletions were included. The fact that patients with exon 21 point mutations (L858R) were not included possibly avoided confounding effects caused by differences in TKI affinity between both mutations. Cell-based studies have shown that EGFR with exon 19 deletions are more sensitive to TKI than L858R EGFR (7, 24). On the other hand, clinical trials have shown highly comparable response rates in both mutations. This suggests that TKIs have sufficient affinity to provoke similar initial tumor responses in both types of mutations. ¹¹C]Erlotinib uptake in patients with exon 21 point mutations is unknown and should be investigated in future studies.

Full kinetic modeling and arterial blood sampling were used to derive the volume of distribution of ¹¹C]erlotinib. This approach provides the most accurate assessment of erlotinib uptake, which is important in the present proof-of-concept study. It is, however, less suitable for routine clinical studies, and further studies are needed to assess simplified

analytic methods, such as the standardized uptake value (SUV). Preliminary data indicate that an SUV analysis provides a poorer discrimination between both patients groups. On the other hand, tumor-to-blood ratios appear to be more promising. A full comparison is in progress. Simplified methods are also relevant for whole body scans, enabling the study of interlesional heterogeneity.

Differences in V_T between both patient groups could potentially be due to differences in nonspecific binding. The nonspecific component of V_T given by K_1/k_2 , however, did not significantly differ between groups. Ideally, this should be confirmed in an independent measurement. One possibility would be to measure V_T after a blocking dose with cold erlotinib. This is, however, not possible in patients and needs to be conducted in future animal studies.

V_T differences between groups appear modest, when compared with the differences in K_i/K_M ratios between mutated and wild-type EGFR. However, V_T values between groups are clearly distinct, with excellent test-retest repeatability, justifying further validation studies with larger numbers of patients, to answer the question whether V_T can be used to effectively distinguish between patients who will and will not benefit from TKI treatment.

In this study, using SPE followed by HPLC, the radioactive parent compound fraction was discriminated from the radioactive metabolite fractions in arterial plasma samples. Clearly, metabolite fractions in tumors were not determined. Previous pharmacology studies have shown that the main metabolite of erlotinib is OSI-420, the precursor to which the C-11 label is introduced in the synthesis of ¹¹C]erlotinib. After losing the C-11 label at the 7-methoxyethoxy position, OSI-420 becomes nonradioactive and does not show up on the PET scan. This metabolism does result in small polar radiolabeled metabolites such as C-11 formaldehyde, C-11 formic acid, and/or C-11 carbon monoxide. These metabolites could cause some bias, that is, an underestimation, of V_T differences between groups.

Biopsies were not taken at the time of scanning, as indicated in Table 1. No biopsies were taken for the purpose of the present study. This is a relevant limitation, especially for patients with exon 19 deletions who were treated with TKI (i.e., patients 7, 8, and 10) before scanning, as they may have developed secondary mutations, for example, T790M, that could decrease the affinity of EGFR for ¹¹C]erlotinib. In patient 7, no secondary mutations were found in biopsies taken 1 month before scanning. This biopsy was considered representative. In addition, to date (i.e., 22 months), this patient has maintained a partial response to erlotinib. Patient 8 and 10 underwent an additional biopsy, revealing the presence of T790M, 6 and 12 months after scanning, respectively, indicating that disease progression was probably due to this secondary mutation. It is believed that T790M mutations are already present in tumor cells with activating mutations, and that during TKI therapy, a clonal selection takes place. This means that both patients 8 and 10 could have had T790M-bearing tumor cells during scanning, but to which extent and how this changed ¹¹C]erlotinib uptake is unclear.

Future perspectives

More studies are needed to validate and substantiate the present findings. In future research, the use of simplified parameters such as SUV should be investigated. In addition, future research needs to focus on heterogeneity in tumor [¹¹C]erlotinib V_T , especially after initiation of TKI therapy and after disease progression occurs. In case of emerging resistance to TKI, [¹¹C]erlotinib PET may reveal residual TKI-sensitive tumor sites, which could justify continuation of TKI within a more complex treatment protocol. As all TKI-treated patients develop resistance, this is an important clinical issue. Furthermore, the use of static whole body [¹¹C]erlotinib scans could provide a means to evaluate distant metastatic lesions and their TKI sensitivity. The present study with [¹¹C]erlotinib can serve as a template for other studies using radiolabeled TKI that target different tyrosine kinases and activate proliferative pathways in a variety of other malignancies.

In conclusion, the present study shows that measuring [¹¹C]erlotinib uptake by V_T using PET is feasible. [¹¹C]erlotinib V_T is higher in patients with NSCLCs with EGFR exon 19 deletions. Therefore, this noninvasive *in vivo* method shows promise as a tool for individualizing therapy by identifying those patients who may benefit from TKI therapy.

Disclosure of Potential Conflicts of Interest

No potential conflicts of interest were disclosed.

References

- Pao W, Miller V, Zakowski M, Doherty J, Politi K, Sarkaria I, et al. EGFR receptor gene mutations are common in lung cancers from "never smokers" and are associated with sensitivity of tumors to gefitinib and erlotinib. *Proc Natl Acad Sci U S A* 2004;101:13306.
- Lynch TJ, Bell DW, Sordella R, Gurubhagavatula S, Okimoto RA, Brannigan BW, et al. Activating mutations in the epidermal growth factor receptor underlying responsiveness of non-small-cell lung cancer to gefitinib. *N Engl J Med* 2004;350:2129–39.
- Maemondo M, Inoue A, Kobayashi K, Sugawara S, Oizumi S, Isobe H, et al. Gefitinib or chemotherapy for non-small-cell lung cancer with mutated EGFR. *N Engl J Med* 2010;362:2380–8.
- Mitsudomi T, Morita S, Yatabe Y, Negoro S, Okamoto I, Tsurutani J, et al. Gefitinib versus cisplatin plus docetaxel in patients with non-small-cell lung cancer harbouring mutations of the epidermal growth factor receptor (WJTOG3405): an open label, randomised phase 3 trial. *Lancet Oncol* 2010;11:121–8.
- Mok TS, Wu YL, Thongprasert S, Yang CH, Chu DT, Saijo N, et al. Gefitinib or carboplatin-paclitaxel in pulmonary adenocarcinoma. *N Engl J Med* 2009;361:947–57.
- Cobo M, Isla D, Massuti B, Montes A, Sanchez JM, Provencio M, et al. Customizing cisplatin based on quantitative excision repair cross-complementing 1 mRNA expression: a phase III trial in non-small-cell lung cancer. *J Clin Oncol* 2007;25:2747–54.
- Carey KD, Garton AJ, Romero MS, Kahler J, Thomson S, Ross S, et al. Kinetic analysis of epidermal growth factor receptor somatic mutant proteins shows increased sensitivity to the epidermal growth factor receptor tyrosine kinase inhibitor, erlotinib. *Cancer Res* 2006;66:8163–71.
- Memon AA, Jakobsen S, Dagnaes-Hansen F, Sorensen BS, Keiding S, Nexø E. Positron emission tomography (PET) imaging with [¹¹C]-labeled erlotinib: a micro-PET study on mice with lung tumor xenografts. *Cancer Res* 2009;69:873–8.
- Memon AA, Weber B, Winterdahl M, Jakobsen S, Meldgaard P, Madsen HHT, et al. PET imaging of patients with non-small cell lung cancer employing an EGF receptor targeting drug as tracer. *Br J Cancer* 2011;105:1850–5.
- Weber B, Winterdahl M, Memon A, Sorensen BS, Keiding S, Sorensen L, et al. Erlotinib accumulation in brain metastases from non-small cell lung cancer: visualization by positron emission tomography in a patient harboring a mutation in the epidermal growth factor receptor. *J Thorac Oncol* 2011;6:1287.
- Heideman D, Thunnissen F, Doeleman M, Kramer D, Verheul H, Smit E, et al. A panel of high resolution melting (HRM) technology-based assays with direct sequencing possibility for effective mutation screening of EGFR and K-ras genes. *Anal Cell Pathol* 2009;31:329–33.
- Kramer D, Thunnissen F, Gallegos-Ruiz M, Smit E, Postmus P, Meijer C, et al. A fast, sensitive and accurate high resolution melting (HRM) technology-based assay to screen for common K-ras mutations. *Anal Cell Pathol* 2009;31:161–7.
- van der Veldt AAM, Hendrikse NH, Harms HJ, Comans EFI, Postmus PE, Smit EF, et al. Quantitative parametric perfusion images using ¹⁵O-labeled water and a clinical PET/CT scanner: test-retest variability in lung cancer. *J Nucl Med* 2010;51:1684.
- Boellaard R, van Lingen A, van Balen SCM, Hoving BG, Lammertsma AA. Characteristics of a new fully programmable blood sampling device for monitoring blood radioactivity during PET. *Eur J Nucl Med Mol Imaging* 2001;28:81–9.
- Lammertsma AA, Bench CJ, Hume SP, Osman S, Gunn K, Brooks DJ, et al. Comparison of methods for analysis of clinical [¹¹C]raclopride studies. *J Cereb Blood Flow Metabol* 1996;16:42–52.
- Schwarz G. Estimating the dimension of a model. *Ann Stat* 1978;6:461–4.
- Akaike. A new look at the statistical model identification. *IEEE Trans Autom Control* 1974;19:716–23.

Authors' Contributions

Conception and design: I. Bahce, E.F. Smit, A.A.M. van der Veldt, A.D. Windhorst, P.E. Postmus, A.A. Lammertsma, N.H. Hendrikse
Development of methodology: I. Bahce, E.F. Smit, M. Lubberink, M. Yaqub, A.D. Windhorst, A.A. Lammertsma
Acquisition of data (provided animals, acquired and managed patients, provided facilities, etc.): I. Bahce, E.F. Smit, R.C. Schuit, E. Thunnissen, D. A.H. Heideman, P.E. Postmus
Analysis and interpretation of data (e.g., statistical analysis, biostatistics, computational analysis): I. Bahce, E.F. Smit, M. Lubberink, A.A.M. van der Veldt, M. Yaqub, A.A. Lammertsma
Writing, review, and/or revision of the manuscript: I. Bahce, E.F. Smit, M. Lubberink, A.A.M. van der Veldt, M. Yaqub, A.D. Windhorst, E. Thunnissen, D.A.H. Heideman, P.E. Postmus, A.A. Lammertsma, N.H. Hendrikse
Administrative, technical, or material support (i.e., reporting or organizing data, constructing databases): A.D. Windhorst, R.C. Schuit, E. Thunnissen, D.A.H. Heideman
Study supervision: E.F. Smit, A.A. Lammertsma, N.H. Hendrikse

Acknowledgments

The authors thank Suzette van Balen and Femke Jongsma for assistance with PET scanning and planning, Ronald Boellaard for advice on tracer kinetic modeling, and the B.V. Cyclotron VU for production and delivery of [¹¹C]CO₂.

Grant Support

This study was conducted within the framework of the Center for Translational Molecular Medicine, Airforce project (grant 03O-103).

The costs of publication of this article were defrayed in part by the payment of page charges. This article must therefore be hereby marked *advertisement* in accordance with 18 U.S.C. Section 1734 solely to indicate this fact.

Received January 28, 2012; revised October 17, 2012; accepted October 17, 2012; published OnlineFirst November 7, 2012.

18. Yaqub M, Boellaard R, Kropholler MA, Lammertsma AA. Optimization algorithms and weighting factors for analysis of dynamic PET studies. *Phys Med Biol* 2006;51:4217–32.
19. Ruiz MIG, Floor K, Steinberg S, Grünberg K, Thunnissen FBJM, Belien JAM, et al. Combined assessment of EGFR pathway-related molecular markers and prognosis of NSCLC patients. *Br J Cancer* 2008;100:145–52.
20. Eisenhauer E, Therasse P, Bogaerts J, Schwartz L, Sargent D, Ford R, et al. New response evaluation criteria in solid tumours: revised RECIST guideline (version 1.1). *Eur J Cancer* 2009;45:228–47.
21. Greulich H, Chen T-H, Feng W, Jänne PA, Alvarez JV, Zappaterra M, et al. Oncogenic transformation by inhibitor-sensitive and -resistant EGFR mutants. *PLoS Med* 2005;2:e313.
22. Logan J, Fowler JS, Volkow ND, Wolf AP, Dewey SL, Schlyer DJ, et al. Graphical analysis of reversible radioligand binding from time-activity measurements applied to [N-11C-methyl]-(-)-cocaine PET studies in human subjects. *J Cereb Blood Flow Metabol* 1990;10:740–7.
23. Visvikis D, Francis D, Mulligan R, Costa D, Croasdale I, Luthra S, et al. Comparison of methodologies for the *in vivo* assessment of 18 FLT utilisation in colorectal cancer. *Eur J Nucl Med Mol Imaging* 2004;31:169–78.
24. Mulloy R, Ferrand A, Kim Y, Sordella R, Bell DW, Haber DA, et al. Epidermal growth factor receptor mutants from human lung cancers exhibit enhanced catalytic activity and increased sensitivity to gefitinib. *Cancer Res* 2007;67:2325–30.
25. Goldstraw P, ed. IASLC staging handbook in thoracic oncology. Orange Park (FL): Editorial Rx Press; 2009.